Quaternary Geochronology 49 (2019) 131–137

Contents lists available at ScienceDirect

Quaternary Geochronology

journal homepage: www.elsevier.com/locate/quageo

Research paper

Luminescence characteristics of quartz from Holocene delta deposits of the Yangtze River and their provenance implications

Xiaomei Nian[a,*], Weiguo Zhang[a], Fengyue Qiu[a], Jintang Qin[b], Zhanghua Wang[a], Qianli Sun[a], Jing Chen[a], Zhongyuan Chen[a], Niankai Liu[c]

[a] State Key Laboratory of Estuarine and Coastal Research, East China Normal University, Shanghai 200062, China
[b] State Key Laboratory of Earthquake Dynamics, Institute of Geology, China Earthquake Administration, Beijing 100029, China
[c] Department of the History of Science, Tsinghua University, Beijing 100084, China

A R T I C L E I N F O

Keywords:
Optically stimulated luminescence (OSL)
Quartz
Luminescence sensitivity
Provenance
Yangtze River delta

A B S T R A C T

The optically stimulated luminescence (OSL) sensitivity and OSL signal components of quartz grains were used to investigate provenance changes of Holocene sediments from the Yangtze River delta. The variation of luminescence sensitivity was observed in multiple grain aliquots and single grains of quartz from different sedimentary units of the Yangtze River delta. Laboratory experiments suggest that repeated dosing/bleaching cycles increase the luminescence sensitivity of quartz from the studied sediments. High variable thermal activation curves were observed even for samples from the same sedimentary unit, implying highly diverse sources for the delta deposits of the Yangtze River. Different sedimentary units show quartz with similar OSL component contributions, and repeated dosing/bleaching cycles and heating treatment are unable to affect the relative contributions of the fast and medium components to the bulk OSL signal. The samples from unit 1 (U1, tidal river, 15–11 ka), unit 2 (U2, estuary, 11–9 ka) and unit 6 (U6, delta plain, ca. 1 ka to the present) show relatively higher luminescence sensitivity in comparison to unit 3 (U3, tidal sand ridge, 9–4 ka), unit 4 (U4, prodelta, 4–2.5 ka) and unit 5 (U5, delta front, 2.5–1 ka), implying changing sediment sources over time. Such a temporal variation of sediment source can be explained by the transgressive/regressive history of the Yangtze River delta as well as by Asian monsoon variability since the last deglaciation. It demonstrates that luminescence sensitivity of quartz has great potential for tracing sediment sources in the Yangtze River delta, but more work is needed to characterize specific sources to establish a source-to-sink linkage.

1. Introduction

In addition to its widespread application in determining burial ages of Quaternary sediments (Aitken, 1998), the luminescence signal of mineral grains has also shown great potential in tracing the provenance of sediments (Li et al., 2002). Much effort has been devoted to the use of quartz luminescence sensitivity for tracing the sources of sediments in deserts (Li et al., 2007; Zheng et al., 2009; Lü and Sun, 2011; Zheng and Zhou, 2012; Gong et al., 2015), including loess sequences (Lü et al., 2014; Qiu and Zhou, 2015). In recent years, the technique has also been used to study the sediment sources of fluvial or coastal deposits (Pietsch et al., 2008; Tsukamoto et al., 2011; Sawakuchi et al., 2011, 2012; do Nascimento et al., 2015; Zular et al., 2015). For example, a study of the southern Brazilian coast showed that sediment source discrimination based on quartz optically stimulated luminescence (OSL) sensitivity is consistent with discrimination using particle size and heavy mineral variables (Sawakuchi et al., 2012; Zular et al., 2015). Luminescence properties of quartz (e.g. sensitivity, thermal activation and signal components) are affected by the parent rock, and therefore quartz from different sources should show different luminescence characteristics (Sawakuchi et al., 2011). However, it was also found that luminescence sensitization of quartz from the same source varies with the cycles of bleaching and irradiation during sediment transport (e.g. Preusser et al., 2006; Fitzsimmons, 2011; Sawakuchi et al., 2011). Therefore, the successful application of OSL sensitivity analysis in sediment source tracing requires a proper assessment of the influence of sediment transport history on OSL sensitization.

The Yangtze River is the world's third largest river with a catchment area of 1.8 million km^2. The present Yangtze River delta has evolved in the context of post-glacial climate change, sea-level change and human activities (e.g. Li and Wang, 1998). There is a buried incised valley on the delta, which was formed during the Last Glacial Maximum and was subsequently infilled by early Holocene transgressive deposits and middle-late Holocene regressive delta deposits (Li et al., 2000). Several

* Corresponding author.
E-mail address: xmnian@sklec.ecnu.edu.cn (X. Nian).

https://doi.org/10.1016/j.quageo.2018.04.010
Received 6 December 2017; Received in revised form 17 April 2018; Accepted 27 April 2018
Available online 30 April 2018

studies have used sediment cores from the incised valley to reconstruct the evolution of the delta (e.g. Wang et al., 1981; Chen and Stanley, 1998; Li et al., 2000; Hori et al., 2001, 2002; Wang et al., 2012; Song et al., 2013; Nian et al., 2018a,b). However, it is unclear whether there were sediment source variations during the Holocene transgression-regression cycle.

In this study, a sediment core from the incised valley of the Yangtze River delta was subjected to quartz luminescence sensitivity measurements (multiple and single grains) and analysis of their thermal activation characteristics and OSL components. The results are used to assess the influence of parent rock and sediment transport history on OSL sensitivity. The principal objective of the study was to investigate the potential of applying quartz luminescence signals in sediment source tracing of Holocene sediments in the Yangtze River delta.

2. Study area and methods

During the low sea-level stand of the late Pleistocene, the Yangtze River was incised to a maximum depth of 70–80 m in the delta region (Li et al., 2000). Since the Last Glacial Maximum, the incised valley accumulated sediment with the rising sea-level, and changed from a fluvial to an estuarine environment, and after the maximum transgression at ~8 ka, the delta began to develop. Based on the seaward migration of river mouth sand-bar deposits, the development of the delta can be divided into six sub-stages: Hongqiao (7.5–6.0 ka or 6.0–5.5 ka; Song et al., 2013), Huangqiao (6.5–4.0 ka), Jinsha (4.5–2.0 ka), Haimen (2.5–1.2 ka), Chongming (1.7–0.2 ka) and Changxing (0.7–0 ka), in geochronological order (Delta Research Group, 1978).

Core NT (32°3.9417′N, 120°51.4′E, 4 m above sea level) (Fig. 1) was divided into six depositional units, labeled U1–U6 in ascending order: tidal river (U1), estuary (U2), tidal sand ridge (U3), prodelta (U4), delta front (U5) and delta plain (U6). These units show a cycle of transgression and regression (Bai et al., 2016; Nian et al., 2018a) (Fig. S1). Lithological descriptions of the core are given in Fig. S1. In this study, 12 samples from the core were used to study the quartz luminescence characteristics, including two samples from each unit to enable cross-checking (Fig. S1).

Coarse-grained quartz (90–125 μm) was extracted from the samples using the following procedure. The samples were first pre-treated with HCl (10%) to remove carbonates, and then with H_2O_2 (30%) to remove organic material, after which they were washed several times with distilled water and sieved to retrieve grains of the size range 90–125 μm. The samples were then treated in HF (40%) for 40 min, and washed in 10% HF to obtain the quartz grains. The purity of the quartz grains was checked using the OSL-IR (infrared) depletion ratios (Duller, 2003) and the 110 °C thermoluminescence (TL) peak (Li et al., 2002). The OSL-IR depletion ratios were between 0.9 and 1.1 for all measured aliquots and single grains.

Luminescence measurements were performed with a Risø-TL/OSL DA-20 reader with an automated detection and stimulation head (DASH) and a calibrated $^{90}Sr/^{90}Y$ beta source for irradiation (dose rates of ca. 0.101 Gy/s and 0.113 Gy/s for multiple-grain aliquots and single grains, respectively). The OSL signal was detected using an ET EMD-9107 photomultiplier tube through a 7.5-mm-thick Hoya U-340 filter. OSL measurements were carried out using a blue LED (470 nm, 90% of the full power, 97 mW cm^{-2}) and IR LED (870 nm, 90% of the full power, 129 mW cm^{-2}) for quartz multiple-grain aliquot measurements, and with a green laser (532 nm, 90% of the full power, 100 mW cm^{-2}) for quartz single grain measurements. Quartz grains were mounted on 9.7-mm diameter aluminum discs using Silkospray silicone oil for multiple-grain aliquot (1–2 mg) measurements. For single grain measurements, the quartz grains were spread over the single-grain disc with holes of 300 μm in both depth and diameter. In this study, OSL signal component analysis was performed using the fitting program in Risø Analyst Version 4.31.7.

For luminescence sensitivity measurements of multiple grains, fifteen aliquots of each sample were bleached with blue light at room temperature for 100 s to remove any remaining natural OSL signals. These aliquots were then given a known (20 Gy) beta dose, preheated at 260 °C for 10 s and optically stimulated at 125 °C for 40 s with blue light. The intensities of 110 °C TL signals were recorded during preheating, and integrated between 60 °C and 120 °C for analysis. The OSL sensitivity was calculated from the integral of the initial 0.4 s of the OSL decay curve dominated by the fast component, after subtracting the background taken as the average of the last 10 s of measurements.

To characterize how quartz OSL sensitivity differed from one sample to another, single grain OSL measurements were carried out. Fifteen single-grain discs for each sample were bleached at room temperature with blue LEDs for 100 s. After bleaching, the quartz grains were irradiated with a beta dose of 22 Gy, preheated at 260 °C for 10 s and stimulated with the green laser for 1 s. Signals from the first 0.085 s (fast component dominated), with the background being obtained from the average of the last 0.17 s, were integrated for analysis.

To test the effects of burial-erosion cycles on the OSL sensitivity resulting from sediment transport, laboratory treatments were performed by repeated dosing/bleaching cycles of the quartz samples. Table 1 shows the protocol used for luminescence measurements with repeated cycles of laboratory irradiation and illumination. There is a strong link between the OSL signal and 110 °C TL peak (Aitken and Smith, 1988), which may result from the same source of trapped charge (Wintle and Murray, 1999). Therefore, only the ratios of observed OSL signal sensitivities following repeated dosing/bleaching measurement were presented to test the effects of cycles on the OSL sensitivity. The regenerative OSL signal in step 8 was normalized to the first measurement in step 4 (Table 1); this is termed the sensitivity ratio (S_n/S_0). In this study, the OSL signal intensity with increasing heating temperature up to 600 °C (the thermal activation measurements) was also measured to evaluate the effect of heating on the OSL sensitivity, using the protocol listed in Table 2.

3. Results

3.1. Luminescence sensitivity of multiple grains

All the OSL and TL intensities were normalized by the mass of each aliquot (signal per dose per mass, counts/mg/Gy). Fig. S2 shows TL and OSL curves representative of quartz samples from each unit. All 12 samples showed TL peaks centered around 90–120 °C and rapidly decaying OSL curves. As illustrated in Fig. 2, the quartz sensitivity shows both intra- and inter-sample variability. In general, quartz from U1 (tidal river), U2 (estuary) and U6 (delta plain) is more sensitive than that from the other units.

3.2. Luminescence sensitivity of single grains

Fig. S3 shows the ratio of summed signal intensities as a function of the proportion of grains with decreasing sensitivity. The distribution of the OSL sensitivity from 1500 quartz single grains for each sample is illustrated in Fig. 3a. From the OSL sensitivity at the single-grain scale, we can see that only a small number of very bright grains contribute a much greater fraction of the total OSL signals, while most of the grains have relatively weak signals (Fig. 3a and S3). This is consistent with previous studies (e.g. Duller and Murray, 2000; Nian et al., 2018b). The grains show substantial sensitivity variability within a single sample, ranging from 0 to 700 counts/Gy. Despite this, it is evident that units 3, 4 and 5 (U3, U4 and U5) generally have a lower variability and median values than those of units 1, 2 and 6 (U1, U2 and U6). The difference between samples of the same unit is larger for units 1, 2 and 4.

3.3. Effects of dosing/bleaching on changes in OSL sensitivity

The effect of dosing/bleaching cycles on the sensitization was tested

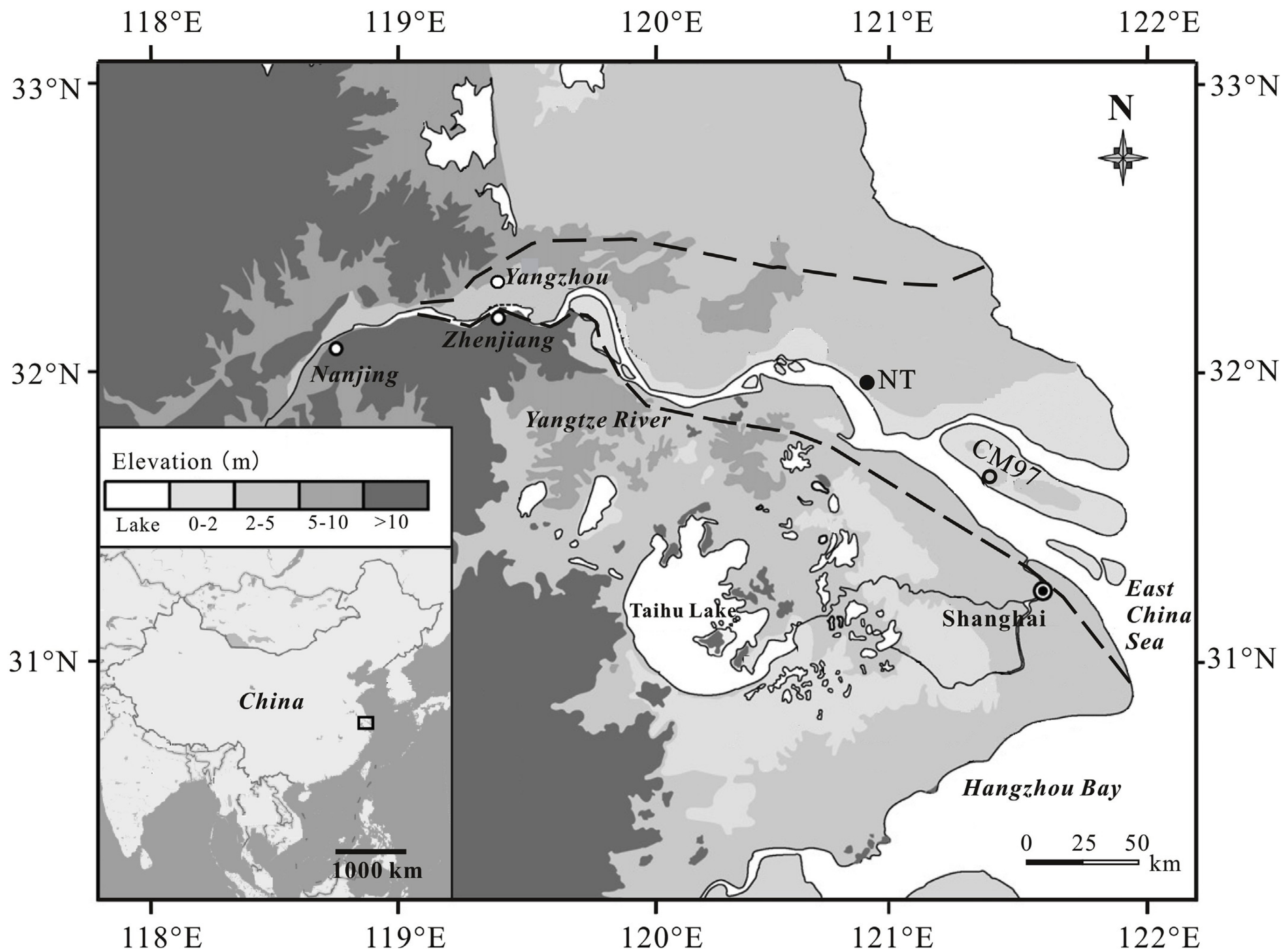

Fig. 1. Study area showing the location of core NT (modified from Bai et al., 2016) and core CM97 mentioned in the text (Bi et al., 2017). The dashed line represents the boundary of the incised valley during the last glacial maximum (after Li et al., 2000).

Table 1
Measurement protocol used for repeated irradiation and bleaching.

Step	Procedure	Observed
1	Blue light bleaching for 100 s at 20 °C	
2	Given dose, 20 Gy	
3	Preheat (260 °C for 10 s)	
4	Stimulate for 40 s at 125 °C	S_0
5[a]	n cycles of dosing/bleaching	n = 2,5,10,15
6	Given dose, 20 Gy	
7	Preheat (260 °C for 10 s)	
8	Stimulate for 40 s at 125 °C	S_n
9	Return to step 5	

[a] Given dose = 20 Gy, while the aliquots were bleached with blue light at 20 °C for 40 s.

Table 2
Protocol used for obtaining the thermal activation curves.

Step	Procedure	Observed
1	Blue light bleaching for 100 s at 20 °C	
2	Heat to T °C (T = 200 °C)	
3	Given dose, 20 Gy	
4	Preheat (260 °C for 10 s)	
5	Stimulate for 40 s at 125 °C	S_n (n = 0,1 …)
6	Return to step 2, and T = T + 40 °C	

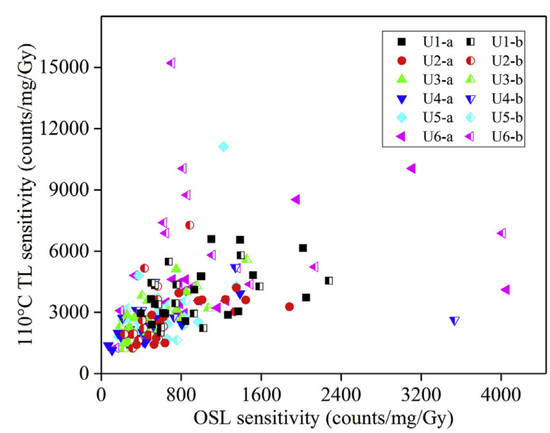

Fig. 2. OSL signal intensity and the intensity of the 110 °C TL peak.

using the protocol summarized in Table 1. The aliquots were successively treated with two, five, ten and fifteen cycles of dosing/bleaching (S_n, Step 5a), that is, there were 32 cycles of dosing/beaching for each aliquot in total, except for the first measurement (S_0, Step 4). Each regenerative OSL signal after different numbers of cycles was normalized to the first measurement (S_0). As shown in Fig. 4a, the S_n/S_0 ratio showed an increase by factors of 1.00–1.18, 1.02–1.41, 1.20–1.72, 1.28–1.95 after two, five, ten and fifteen cycles of dosing and bleaching,

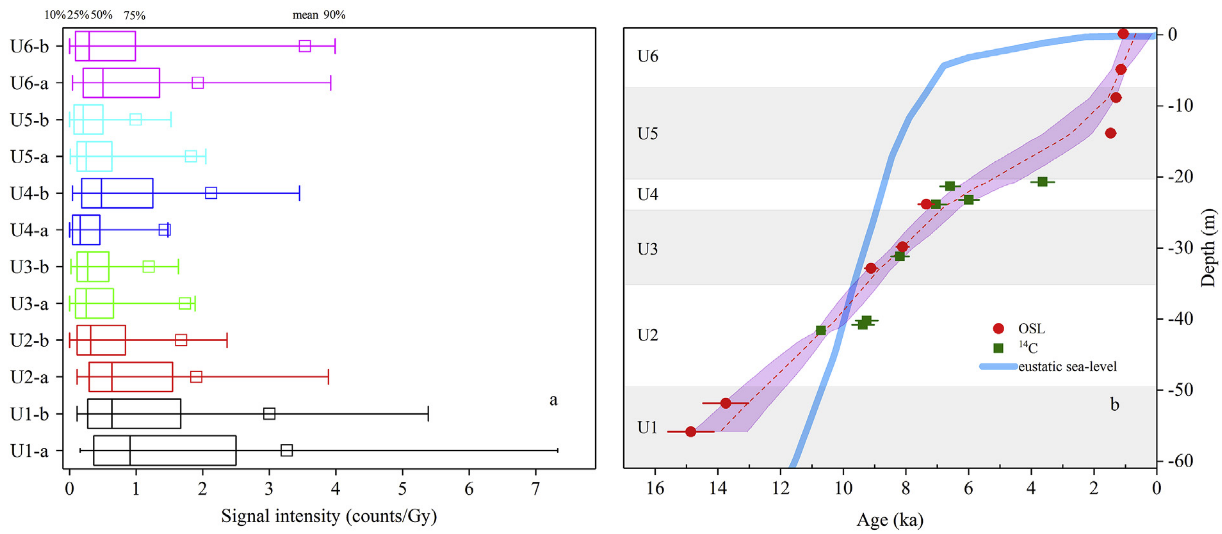

Fig. 3. a) Box and whisker plots of quartz single-grain OSL intensities for 12 samples from core NT. b) Age-depth plot for core NT core (Nian et al., 2018a) and eustatic sea-level curve (Lambeck et al., 2014). The age-depth model was constructed using Bacon age-modelling software (Blaauw and Christen, 2011). The pink shaded area is the 95% probability interval, and the red dotted line indicates the single 'best' age-depth model from the weighted average age.

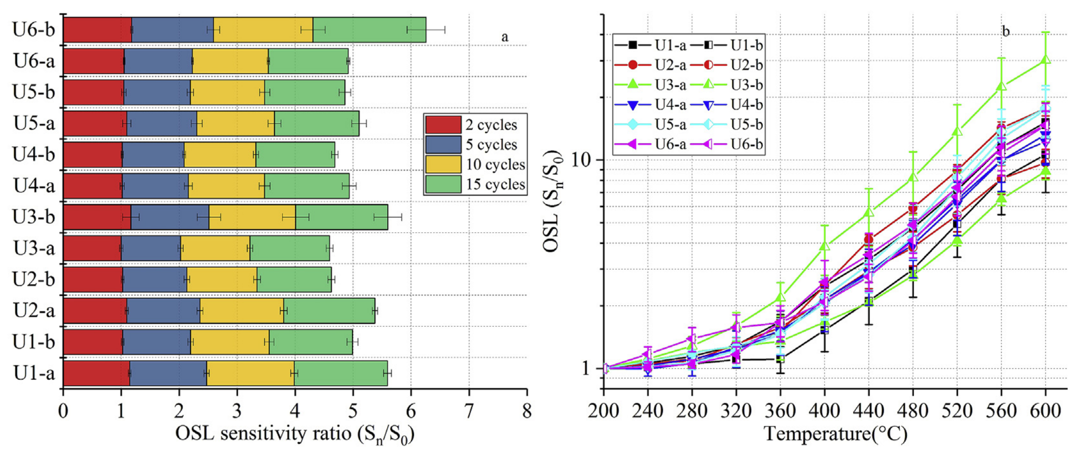

Fig. 4. a) OSL sensitivity ratios versus repeated dosing/bleaching cycles. Each regenerative OSL signal was normalized to the first measurement (S_0, Table 1, step 4). b) OSL sensitivity ratio as a function of increasing heating temperature. Each regenerative OSL signal was normalized to the first measurement (S_0, Table 2, step 5). All the data are presented as the average value of 4–6 aliquots for each sample.

respectively. The OSL signal sensitivities increased slowly with increasing cycle number, with samples U3-b and U6-b having the maximum values.

3.4. Thermal activation curves (TAC)

The thermal activation characteristics of the OSL signals were investigated using the protocol summarized in Table 2. The regenerative OSL signals (S_n, step 5) after heat treatments (from 200 °C to 600 °C in 40 °C increments) were normalized to the first measurement (S_0, after the first 200 °C heat treatment). The normalized signals were termed OSL sensitivity ratios (S_n/S_0). As shown in Fig. 4b, different behaviors of thermal activation characteristics were found for quartz samples from different units, even for samples from the same unit. The OSL sensitivity ratios increased slowly until the heating temperature of 360 °C, and then the ratios showed a rapid increase from 360 °C to 600 °C. The ratios for the samples from unit 4–6 showed a similar tendency of sensitization; the largest internal differences were found for the samples from units 1–3. Samples U3-a and U3-b displayed the smallest and largest growth ratios by 600 °C, which are factors 9 and 30, respectively (Fig. 4b).

3.5. Comparison of OSL components

In the present study, three exponential signal components were fitted to the OSL decay curves (Table 1, step 4), corresponding to the fast, medium and slow components (Smith and Rhodes, 1994; Bailey et al., 1997). The fast component dominated the initial CW-OSL signal (0–0.1 s) of quartz for single aliquots measurements, and the slow component was very weak (Fig. 5). Typically, the contributions of the fast, medium and slow components to the net OSL signals of the studied samples were 80–97%, 3–20%, and < 3%, respectively. However, it is difficult to distinguish the studied units from the relative contributions of the quartz OSL components.

To test the effect of dosing/bleaching on OSL components, three components were fitted to the OSL signals (Table 1, step 4 and 8). A typical example for samples from unit 1 is shown in Fig. 6a, and the ratios for all the samples are plotted in Fig. S4. Evidently, repeated dosing/bleaching cycles did not change the components of the quartz OSL signals, and the proportions of the different components were overall stable with repeated cycles. The OSL signal was dominated by the fast component for these samples.

To test the effect of heating on OSL components, three exponential components were fitted to the OSL signals (Table 2, step 5). As shown in

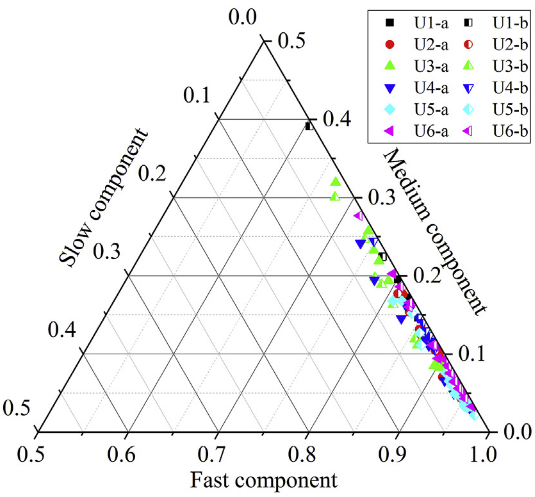

Fig. 5. Ternary diagram showing the relative contributions of different quartz OSL components for the samples from the Yangtze River delta. Fifteen aliquots were used for each sample.

Fig. 6b (unit 1) and Fig. S5, the heating temperature also had no apparent impact on the OSL components of quartz, and the fast component still made up the dominant proportion of the signals.

4. Discussion

4.1. Effects of sediment source vs. transport history on OSL sensitivity

Our samples show a large variability in OSL sensitivity among different stratigraphic units. In addition, there is also significant variability for samples within the same unit as well as among grains from the same sample (Figs. 2 and 3a). Quartz sensitivities are influenced by sediment source as well as by transport-deposition processes. The OSL signal sensitivity ratios of our samples changed from ca. 1.00 to 1.95 after four different repeating cycles, and increased with increasing cycle number (Fig. 4a). Previous studies also suggested that the sensitivity of quartz may increase in response to repeated cycles of irradiation and bleaching during sediment transport processes (e.g. Preusser et al., 2006; Pietsch et al., 2008). There were a limited number of dosing/bleaching cycles in the laboratory test performed in this study, while quartz grains in nature will likely experience many more cycles during source to sink transport. It seems that transport-deposition processes do have an impact on the sensitivities of the samples.

However, the influence of parent rock on quartz OSL sensitivity cannot be excluded. A marked variation in the shape of TAC (Fig. 4b) can be observed. The shape of the TAC as an intrinsic index of luminescence properties of quartz depends on quartz genesis and therefore parent rock (Aitken, 1985; Kiyak et al., 2008; Zheng et al., 2009). The Yangtze River is a large river with a large number of tributaries (49 rivers with a catchment area > 10,000 km^2) distributed over a catchment area of 1.8 million km^2. The rock type varies greatly over the catchments, including igneous, metamorphic, sedimentary rocks and Quaternary unconsolidated sediments (Zhang et al., 1996). As a result, fluvial sediments from different tributaries show significant variations in geochemical (Yang et al., 2007, Yang and Wang, 2011), magnetic (Zhang et al., 2008; Chen, 2009) and mineralogical compositions (Wang et al., 2006; He et al., 2013). In addition, sediments derived from marine sources may contribute to the delta buildup. Thus, the delta deposits comprise sediments from different tributaries and marine sources. The observed large variations in the form of TAC imply diverse sources of sediments supplied to the Yangtze River delta. This can potentially explain the OSL sensitivity variability of quartz grains within the same sample (Figs. 2 and 3).

4.2. Feasibility of component analysis in sediment tracing

Different components of the quartz OSL signal have different characteristics in terms of the decay rate, and the relative proportions of signal components may differ between quartz grains from different sources (Kuhns et al., 2000). In previous studies on desert sands, quartz OSL components were found to vary with sediment source (e.g. Zheng et al., 2012; Gong et al., 2015). By fitting the OSL decay curves after repeated dosing/bleaching cycles, we found that the relative proportion of the individual components did not change with cycles (Fig. 6a and S4). These results are consistent with those of an investigation of sand dunes in China (Gong et al., 2015). In addition, the relative contributions of different components to the total signal apparently do not change as a function of heating temperature, and exhibit a thermal stability (Fig. 6b and S5). As shown in Figs. 5 and 6, S4 and S5, the fast component dominates quartz OSL signals for samples from the study area, which might lead to a smaller potential increment of the contribution of the fast component to the bulk OSL signal during laboratory dosing/bleaching cycles and heating. In general, we did not find differences in component contributions among the different samples, implying that component analysis is not applicable to sediment tracing in the study area.

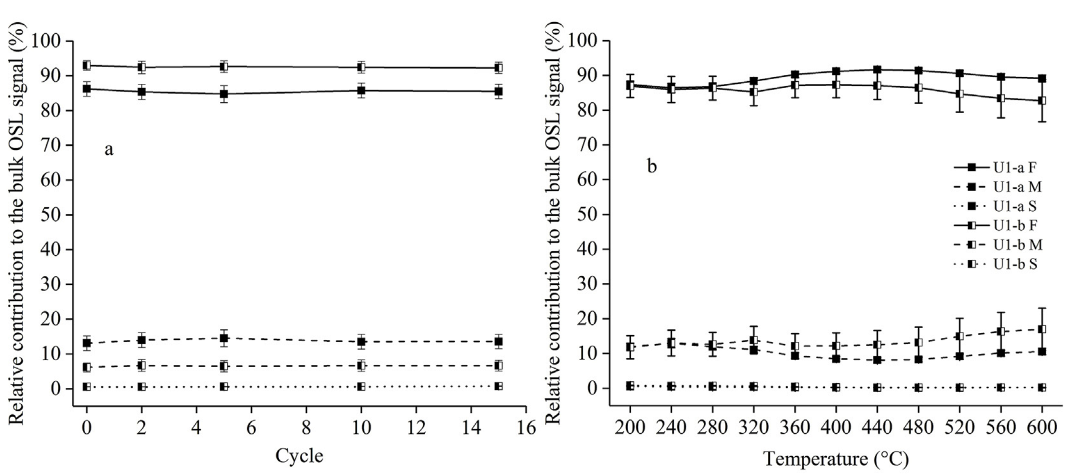

Fig. 6. Examples of the relative contribution of the individual components to the bulk OSL signal (0–0.1 s) for the samples from different units after repeated dosing/bleaching cycles (a) and heating at different temperatures (b). F: fast component; M: medium component; S: slow component.

4.3. Implications of OSL sensitivity for changes in sediment source

Several studies have shown that large river delta deposits experience sediment source changes, including the Mississippi and Nile deltas (Montero-Serrano et al., 2010; Hennekam et al., 2015). Such a sediment source change is linked to the intensity and location of the precipitation regime and landcover within catchments with varied parent rocks, which is further influenced by Holocene climate change. Considering the huge area of the Yangtze River catchment and the variability of the Asian monsoon since the late Pleistocene (Rao et al., 2016; Zhu et al., 2017), changes in sediment sources for the Yangtze River delta would be expected. In an investigation of Sr-Nd isotopic records of a neighboring core CM 97 (Fig. 1), Bi et al. (2017) found that the provenance of sediments in the Yangtze River delta changed from the upper catchment during the late Pleistocene to the mid-lower valley in the early-mid Holocene and the upper catchment again during the late Holocene. They suggested that the changes during the first two periods were controlled by changes in rainfall associated with the evolution of the Indian and East Asian summer monsoons, while the change during the late Holocene was caused by intensified human activity.

Despite the variability of quartz sensitivity within samples, the samples from units U1 (tidal river, 15–11 ka), U2 (estuary, 11–9 ka) and U6 (delta plain, ca. 1 ka) exhibited relatively high luminescence sensitivity compared with the samples from units 3–5 (U3–U5) (Figs. 2b and 3a). Such a temporal change in OSL sensitivity roughly matches the temporal variations of Nd isotopes in core CM97 (Bi et al., 2017). It further supports the explanation of variations in OSL sensitivity in terms of sediment source. The quartz OSL signals for the samples from units U1 and U2 show different luminescence sensitivities compared with the samples from U6 (Figs. 3a and 4). According to our previous study (Nian et al., 2018a), U1 and U2 were formed from the last deglaciation to early Holocene, when the rate of eustatic sea-level rise increased rapidly (Bard et al., 1996) (Fig. 3b). U1 and U2 were formed in the Holocene transgressive stage of the delta, when sediments of the marine source could be transported landward with the rising sea-level. U3 to U5 were formed during the regressive stage of the delta. Fluvial sediments were the main component of the delta deposits; however, the coring site was far from the depocenter and therefore it experienced a lower sedimentation rate (Hori and Saito, 2007; Nian et al., 2018a). U6 was formed over the last 1 ka when the depocenter of the delta migrated to the coring site, which thus experienced a higher sedimentation rate. Although both U3–U5 and U6 were formed in the regressive stage, the Holocene Asian monsoon variability and therefore precipitation pattern (Wang et al., 2008; Rao et al., 2016; Zhu et al., 2017) may have caused variations in the amount and composition of fluvial sediments delivered to the study site. In addition, during the period from 1128 to 1855 AD, the Yellow River discharged into the Yellow Sea, which could deliver sediment to the delta via southward-flowing coastal currents (Zhang, 1984).

It should be noted that we cannot identify the specific sources of sediments in core NT core with the present data, considering the complexity in rock types in the huge catchments of the Yangtze River, as well as the influence of marine-sourced sediments. More research is needed to investigate the luminescence characteristics of sediments from the different tributaries and the marine environment. Geochemical and mineralogical characterization can also be performed to further constrain the sediment source information of OSL signals.

5. Conclusions

The luminescence characteristics of quartz OSL signals were investigated to trace the sources of Holocene Yangtze delta sediments. Our results indicate that quartz OSL sensitivity varies between different stratigraphic units. Repeated dosing/bleaching cycles influenced the OSL sensitivity, suggesting that transport-deposition processes are at least partially responsible for the sensitivity variations among the samples. However, the variations in the form of TAC imply that sediment source plays a role in the variation of OSL sensitivity. The variability of TAC within the same depositional units underlines the complexity of sediment provenances in the Yangtze River delta, which is consistent with the large size of the Yangtze River together with the multiple tributaries as well as with marine sediment input to the delta deposits. In contrast, OSL components vary little with depositional facies, implying their limited use for sediment source tracing in the study area. From the temporal variations in OSL sensitivities, we found that sediment source change occurred during 15–9 ka, 9–1 ka and the last 1 ka. This three-stage change corresponds to the Holocene transgressive/regressive history as well as to variations in the Asian monsoon.

Acknowledgments

We thank the anonymous referee for helpful comments that greatly improved the quality of the manuscript, and Jan Blomendal for language improvement. This research was supported by the National Natural Science Foundation of China (grants 41771009, 41302135, 41271223), the Postdoctoral Special Science Foundation of China (grant 2017T100284), the Postdoctoral Science Foundation of China (grant 2015M571521), and the State Key Laboratory Special Fund (grants 2014RCDW02, SKLEC-2012KYYW01).

Appendix A. Supplementary data

Supplementary data related to this article can be found at http://dx.doi.org/10.1016/j.quageo.2018.04.010.

References

Aitken, M.J., 1985. Thermoluminescence Dating. Academic Press, London.
Aitken, M.J., 1998. An Introduction to Optical Dating. Oxford University Press, New York.
Aitken, M.J., Smith, B.W., 1988. Optical dating: recuperation after bleaching. Quat. Sci. Rev. 7, 387–393.
Bai, X.X., Zhang, W.G., Dong, Y., Pan, D.D., Wang, Z.H., Sun, Q.L., Chen, J., Chen, Z.Y., Liu, J.Y., 2016. Magnetic properties of Holocene tidal flats in the Yangtze delta and their paleoenvironmental implications. Acta Sedimentol. Sin. 34, 1165–1175 (in Chinese with English abstract).
Bailey, R.M., Smith, B.W., Rhodes, E.J., 1997. Partial bleaching and the decay form characteristics of quartz OSL. Radiat. Meas. 27, 123–136.
Bard, E., Hamelin, B., Arnold, M., Montaggioni, L., Cabioch, G., Faure, G., Rougerie, F., 1996. Deglacial sea-level record from Tahiti corals and the timing of global meltwater discharge. Nature 382, 241–244.
Bi, L., Yang, S.Y., Zhao, Y., Wang, Z.B., Dou, Y.G., Li, C., Zheng, H.B., 2017. Provenance study of the Holocene sediments in the Changjiang (Yangtze River) estuary and inner shelf of the East China sea. Quat. Int. 441, 147–161.
Blaauw, M., Christen, J.A., 2011. Flexible paleoclimate age-depth models using an autoregressive gamma process. Bayesian Anal. 6, 457–474.
Chen, X., 2009. Characteristics of Sediments from the Main Tributaries of the Yangtze River and Their Implication for the Provenance Identification of the Sediments of the Yangtze Estuary. The Master Dissertation of East China Normal University, Shanghai, China.
Chen, Z.Y., Stanley, D.J., 1998. Rising sea level on eastern China's Yangtze delta. J. Coast Res. 14, 360–366.
Delta Research Group, Department of Marine Geology, Tongji University, 1978. Holocene formation and development of the Yangtze delta. Chin. Sci. Bull. 35, 310–313 (in Chinese).
do Nascimento, D.R., Sawakuchi, A.O., Guedes, C.C.F., Giannini, P.C.F., Grohmann, C.H., Ferreira, M.P., 2015. Provenance of sands from the Amazon and Madeira rivers based on detrital heavy minerals and luminescence of quartz and feldspar. Sediment. Geol. 316, 1–12.
Duller, G.A.T., 2003. Distinguishing quartz and feldspar in single grain luminescence measurements. Radiat. Meas. 37, 161–165.
Duller, G.A.T., Murray, A.S., 2000. Luminescence dating of sediments using individual mineral grains. Geologos 5, 88–106.
Fitzsimmons, E.K., 2011. An assessment of the luminescence sensitivity of Australian quartz with respect to sediment history. Geochronometria 38, 199–208.
Gong, Z.J., Sun, J.M., Lü, T.Y., Tian, Z.H., 2015. Investigating the optically stimulated luminescence dose saturation behavior for quartz grains from dune sands in China. Quat. Geochronol. 22, 137–143.
He, M.Y., Zheng, H.B., Huang, X.T., Jia, J.T., Li, l., 2013. Yangtze River sediments from source to sink traced with clay mineralogy. J. Asian Earth Sci. 69, 60–69.
Hennekam, R., Donders, T.H., Zwiep, K., de Lange, G.J., 2015. Integral view of Holocene precipitation and vegetation changes in the Nile catchment area as inferred from its delta sediments. Quat. Sci. Rev. 130, 189–199.

Hori, K., Saito, Y., 2007. An early Holocene sea-level jump and delta initiation. Geophys. Res. Lett. 34, L18401.

Hori, K., Saito, Y., Zhao, Q.H., Cheng, X.R., Wang, P.X., Sato, Y., Li, C.X., 2001. Sedimentary facies of the tide-dominated paleo-Changjiang (Yangtze) estuary during the last transgression. Mar. Geol. 177, 331–351.

Hori, K., Saito, Y., Zhao, Q.H., Wang, P.X., 2002. Evolution of the coastal depositional systems of the Changjiang (Yangtze) River in response to late Pleistocene-Holocene sea-level changes. J. Sediment. Res. 72, 884–897.

Kiyak, N.G., Polymeris, G.S., Kitis, G., 2008. LM-OSL thermal activation curves of quartz: relevance to the thermal activation of the 110°C TL glow-peak. Radiat. Meas. 43, 263–268.

Kuhns, C.K., Larsen, N.A., McKeever, S.W.S., 2000. Characteristics of LM-OSL from several different types of quartz. Radiat. Meas. 32, 413–418.

Lambeck, K., Rouby, H., Purcell, A., Sun, Y.Y., Sambridge, M., 2014. Sea level and global ice volumes from the last glacial maximum to the Holocene. Proc. Natl. Acad. Sci. U.S.A. 111, 15296–15303.

Li, C.X., Chen, Q.Q., Zhang, J.Q., Yang, S.Y., Fan, D.D., 2000. Stratigraphy and paleoenvironmental changes in the Yangtze delta during late quaternary. J. Asian Earth Sci. 18, 453–469.

Li, C.X., Wang, P.X., 1998. Late Quaternary Stratigraphy of the Changjiang Delta. China Science Press, Beijing (in Chinese).

Li, S.H., Chen, Y.Y., Li, B., Sun, J.M., Yang, L.R., 2007. OSL dating of sediments from deserts in Northern China. Quat. Geochronol. 2, 23–28.

Li, S.H., Sun, J.M., Zhao, H., 2002. Optical dating of dune sands in the northeastern deserts of China. Palaeogeogr. Palaeoclimatol. Palaeoecol. 181, 419–429.

Lü, T.Y., Sun, J.M., 2011. Luminescence sensitivities of quartz grains from eolian deposits in northern China and their implications for provenance. Quat. Res. 76, 181–189.

Lü, T.Y., Sun, J.M., Li, S.H., Gong, Z.J., Xue, L., 2014. Vertical variations of luminescence sensitivity of quartz grains from loess/paleosol of Luochuan section in the central Chinese Loess Plateau since the last interglacial. Quat. Geochronol. 22, 107–115.

Montero-Serrano, J.C., Bout-Roumazeilles, V., Sionneau, T., Tribovillard, N., Bory, A., Flower, B.P., Billy, I., 2010. Changes in precipitation regimes over North America during the Holocene as recorded by mineralogy and geochemistry of Gulf of Mexico sediments. Global Planet. Change 74, 132–143.

Nian, X.M., Zhang, W.G., Wang, Z.H., Sun, Q.L., Chen, J., Chen, Z.Y., 2018a. Optical dating of Holocene sediments from the Yangtze River (Changjiang) delta, China. Quat. Int. 467, 251–263.

Nian, X.M., Zhang, W.G., Wang, Z.H., Sun, Q.L., Chen, J., Chen, Z.Y., Hutchinson, S.M., 2018b. The chronology of a sediment core from incised valley of the Yangtze River delta: comparative OSL and AMS ^{14}C dating. Mar. Geol. 395, 320–330.

Pietsch, T.J., Olley, J.M., Nanson, G.C., 2008. Fluvial transport as a natural luminescence sensitiser of quartz. Quat. Geochronol. 3, 365–376.

Preusser, F., Ramseyer, K., Schluchter, C., 2006. Characterisation of low OSL intensity quartz from the New Zealand Alps. Radiat. Meas. 41, 871–877.

Qiu, F.Y., Zhou, L.P., 2015. A new luminescence chronology for the Mangshan loess-palaeosol sequence on the southern bank of the Yellow River in Henan, central China. Quat. Geochronol. 30, 24–33.

Rao, Z., Li, Y., Zhang, J., Jia, G., Chen, F., 2016. Investigating the long-term palaeoclimatic controls on the δD and $\delta^{18}O$ of precipitation during the Holocene in the Indian and East Asian monsoonal regions. Earth Sci. Rev. 159, 292–305.

Sawakuchi, A.O., Blair, M.W., DeWitt, R., Faleiros, F.M., Hyppolito, T., Guedes, C.C.F., 2011. Thermal history versus sedimentary history: OSL sensitivity of quartz grains extracted from rocks and sediments. Quat. Geochronol. 6, 261–272.

Sawakuchi, A.O., Guedes, C.C.F., Dewitt, R., Giannini, P.C.F., Blair, M.W., Nascimento Jr., , Faleiros, F.M., 2012. Quartz OSL sensitivity as a proxy for storm activity on the southern Brazilian coast during the Late Holocene. Quat. Geochronol. 13, 92–102.

Smith, B.W., Rhodes, E.J., 1994. Charge movements in quartz and their relevance to optical dating. Radiat. Meas. 23, 329–333.

Song, B., Li, Z., Saito, Y., Okuno, J., Li, Z., Lu, A.Q., Hua, D., Li, J., Li, Y.X., Nakashima, R., 2013. Initiation of the Changjiang (Yangtze) delta and its response to the mid-Holocene sea level change. Palaeogeogr. Palaeoclimatol. Palaeoecol. 388, 81–97.

Tsukamoto, S., Nagashima, K., Murray, A.S., Tada, R., 2011. Variations in OSL components from quartz from Japan sea sediments and the possibility of reconstructing provenance. Quat. Int. 234, 182–189.

Wang, J.T., Guo, X.M., Xu, S.Y., Li, P., Li, C.X., 1981. Evolution of the Holocene Changjiang delta. Acta Geol. Sin. 55, 67–81 (in Chinese with English abstract).

Wang, Y.J., Cheng, H., Edwards, R.L., Kong, X.G., Shao, X.H., Chen, S.T., Wu, J.Y., Jiang, X.Y., Wang, X.F., An, Z.S., 2008. Millennial- and orbital-scale changes in the East Asian monsoon over the past 224,000 years. Nature 451, 1089–1093.

Wang, Z.B., Yang, S.Y., Li, P., Li, C.X., Cai, J.G., 2006. Detrital mineral compositions of the Changjiang River sediments and their tracing implications. Acta Sedimentol. Sin. 24, 570–578 (in Chinese with English abstract).

Wang, Z.H., Zhuang, C.C., Saito, Y., Chen, J., Zhan, Q., Wang, X.D., 2012. Early mid-Holocene sea-level change and coastal environmental response on the southern Yangtze delta plain, China: implications for the rise of Neolithic culture. Quat. Sci. Rev. 35, 51–62.

Wintle, A.G., Murray, A.S., 1999. Luminescence sensitivity changes in quartz. Radiat. Meas. 30, 107–118.

Yang, S.Y., Jiang, S.Y., Ling, H.F., Xia, X.P., Sun, M., Wang, D.J., 2007. Sr-Nd isotopic compositions of the Changjiang sediments: implications for tracing sediment sources. Sci. China Ser. D 50, 1556–1565.

Yang, S.Y., Wang, Z.B., 2011. Rare Earth element compositions of the sediments from the majortributaries and the main stream of the Changjiang River. Bull. Miner. Petrol. Geochem. 30, 31–39 (in Chinese with English abstract).

Zhang, L.C., She, Z.S., Zhang, S., 1996. Water Environmental Chemical Elements Research. China Environmental Science Press, Beijing (in Chinese).

Zhang, R.S., 1984. Land-forming history of the Huanghe River delta and coastal plain of North Jiangsu. Acta Geograph. Sin. 39, 173–184 (in Chinese).

Zhang, W.G., Xing, Y., Yu, L.Z., Feng, H., Lu, M., 2008. Distinguishing sediments from the Yangtze and Yellow Rivers, China: a mineral magnetic approach. The Holocene 18, 1139–1145.

Zheng, C.X., Zhou, L.P., 2012. Further investigations of quartz luminescence signals as a tool for dust source tracing. Quat. Sci. 32, 1036–1045 (in Chinese with English abstract).

Zheng, C.X., Zhou, L.P., Qin, J.T., 2009. Difference in luminescence sensitivity of coarse-grained quartz from deserts of Northern China. Radiat. Meas. 44, 534–537.

Zhu, Z., Feinberg, J.M., Xie, S., Bourne, M.D., Huang, C., Hu, C., Cheng, H., 2017. Holocene ENSO-related cyclic storms recorded by magnetic minerals in speleothems of central China. Proc. Natl. Acad. Sci. U.S.A. 114, 852–857.

Zular, A., Sawakuchi, A.O., Guedes, C.C.F., Giannini, P.C.F., 2015. Attaining provenance proxies from OSL and TL sensitivities: coupling with grain size and heavy minerals data from southern Brazilian coastal sediments. Radiat. Meas. 81, 39–45.